ORIGINAL PAPER

Very small calcifications are detected and scored in the coronary arteries from small voxel MDCT images using a new automated/calibrated scoring method with statistical and patient specific plaque definitions

Ben A. Arnold · Ping Xiang · Matthew J. Budoff · Song Shou Mao

Abstract A negative (zero) Agatston coronary calcium score (CCS) by current methods confers a very low risk for hard coronary events during the next years. However, controversy remains on how to use a negative score since some hard events still occur. We report on a new method with improved detection sensitivity for very small calcifications with the potential to more confidently rule out early atherosclerotic disease. Seventy-eight (78) patients with negative Agatston scores by conventional methods with 2.5 mm slices were selected from routine GE 64 MDCT scans. Each scan was reconstructed a second time from the same data to create 0.625 mm isotropic voxels. The 2.5 mm images were manually scored by the usual Agatston method using the GE SmartScore™ software. Both the 2.5 and 0.625 mm image sets were scored with a new automated and calibrated method (N-vivo™, Image Analysis). The software automatically computes dual scoring thresholds that are statistically defined and specific for each patient, scanner, and scan. The images were hybrid calibrated by simultaneous scanned phantoms in combination with in vivo blood/muscle references. The output reported the calibrated mass scores along with the number of plaques using 18 pt, 3-D connectivity criteria. A CCS Test phantom with known CaHA microspheres was used to validate the method. Twenty-three percent (18 of 78) of the patients with negative Agatston scores by the conventional method scored positive for coronary calcifications by the N-vivo method. The number of small plaques scored per patient varied from 1 to 4. One patient with a single small calcification suffered a hard coronary event during the CT scan. All of the detected plaques were located in the proximal heart. The conventional CCS method misclassified 23% of these patients as having negative coronary calcium scores. The N-vivo automated scoring method with small voxel CT images increased the detection sensitivity of small calcifications with no increase in radiation dose. Detection of small coronary calcified plaques occult to conventional scoring methods may increase the negative predictive power of calcium scoring and may improve plaque composition analysis.

Keywords Coronary calcium scoring · Calcified plaque · Calibrated calcium scoring · MDCT imaging

B. A. Arnold (✉) · P. Xiang
Image Analysis, 1380 Burkesville Rd, Columbia, KY 42728, USA
e-mail: arnold@image-analysis.com

M. J. Budoff · S. S. Mao
Division of Cardiology, Los Angeles Biomedical Research Institute at Harbor-UCLA, Torrance 90502, CA, USA

Introduction

Detection of the atherosclerotic process at an earlier stage provides improved opportunities for

preventative measures or treatment of this leading cause of death. A zero coronary calcium score (CCS) or the absence of detected calcifications by CT conveys a very low risk for future coronary events and a low probability for non-calcified plaque detection by CT angiography (CTA). However, some hard events due occur in the next few years and plaque is found in some of these patients by CTA. Whether a negative score can be used to rule out disease with sufficient confidence to eliminate further testing remains an important question. It is clinically apparent that discernable small calcifications are frequently presence in cardiac scans that fall below the 130 HU Agatston threshold and fail to score by current methods. The reporting of coronary calcium scores has developed from over 18 years of clinical experience primarily by using the conventional Agatston method with 2.5 or 3 mm slice thicknesses resulting in voxel volumes of approximately 1 mm^3 [1]. Numerous CT studies have shown nevertheless that CCS with these large voxels and current methods correlates highly with the severity of atherosclerotic plaque burden and increased cardiovascular risk [2]. Our preliminary work indicated that advanced methods are required to detect the small calcifications that are frequently missed with the Agatston method [3, 4]. The clinical value of detecting very small vascular calcifications that are missed by current CCS methods is not known.

Using micro-proton beam techniques with sub-micrometer resolution, Roijers et al. [5] demonstrated that coronary arteries already contain micrometer size calcifications at a pre-atheroma stage of the atherosclerotic process. Several histological and micro-CT studies have reported the presence of cellular and sub cellular calcifications in the necrotic cores and fibrous caps of atherosclerotic lesions [6–12]. It is recognized that small calcifications are very difficult to detect even with intravascular imaging and that IVUS may detect only a small fraction of these compared to larger plaques [13–17]. The basic pathology of an atherosclerotic lesion includes a core contains a mixture of extracellular lipid particles, macrophages, and foam cells (the atheroma) and micro calcifications, connective tissue and blood components. The finite size of CT voxels results in partial volume averaging of small calcifications with the other lesion components resulting in reduced peak voxel intensity,

especially with the larger 1-mm^3 voxels of current methods. It may be possible to extract additional diagnostic information by detecting smaller calcifications and more fully characterizing plaque morphology, distribution, and rate of progression. We have been working for several years to develop advanced plaque analysis methods with the goals of achieving higher sensitivity, accuracy, precision and standardization among different CT scanners, scans, and patients [18, 19].

CT scanner HU values are known to vary from scanner drift, tube changes, manufacture software, table height, slice thickness, FOV, kVp, filtration, and other scan parameters [20]. In addition, although not as well recognized, HU values vary dependent on the patient's physical composition including size, shape and bone/muscle/fat ratios in the scan plane. HU values are known to be inaccurate or inconsistent except in idealized, circular, water equivalent phantoms. Water calibrations produce HU values for soft tissues including muscle and fat that are relatively accurate since they contain similar z-values and attenuations as water. This is not true for bone and calcium that are more energy dependent and not well calibrated with water. Current calcium scoring methods typically use a fixed scoring threshold of 130 HU and multiplier thresholds of 200, 300, and 400 based on uncalibrated HU values. Agatston calcium scores are strongly dependent on the thresholds and these are subject to the variations of the uncalibrated HU values. Variability among scanners, software methods, patients, and scan parameters therefore limit the standardization, accuracy, and precision of calcium scores. Because of these and other limitations, a new coronary calcium scoring program was developed which uses automated scoring, automated simultaneous phantom and Hybrid calibrations, dual thresholds, mass scores, and statistical plaque definitions (N-vivo™ Version 1.15, Image Analysis, Inc).

The purpose of the current study was to evaluate the detection sensitivity for very small coronary calcifications of this new, automated calcium scoring method with advanced features. After validating the new method with a CCS test phantom containing small calcium hydroxyapatite (CaHA) microspheres, it was compared to a conventional Agatston scoring method in a small cohort of clinical patients.

Methods and materials

Overview of the N-vivo calcium scoring method

Hybrid calibration

In order to overcome the inaccuracies and variability of HU values as discussed above, an automated Hybrid calibration method was developed which is patient, scanner, and technique specific. The Hybrid method uses both the simultaneously scanned calibration phantom and an additional in vivo calibration from the patients' tissues, blood or muscle/fat as described in more detail elsewhere [18]. Figure 1 shows a representative patient image including the Image Analysis INTable^{TM} calibration phantom pad. The round calibration samples contain calcium hydroxyapatite (CaHA) concentrations of 0, 75 and 150 mg/cc and are torso length. The calibration pad was designed with the small samples encased within the pad to replace standard CT table pads and remain on the scanner table at all times for calibration of any scan.
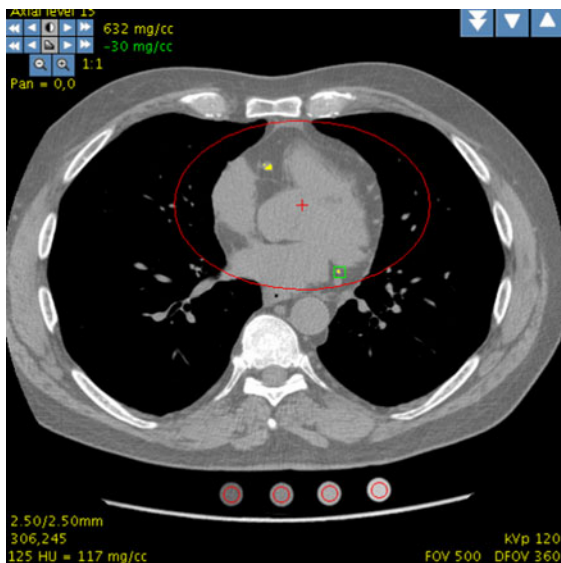

Fig. 1 CT image showing the INTable^{TM} calibration phantom samples positioned under and scanned simultaneously with the patient. Coronary calcifications are automatically detected and highlighted. The *small green box* shows a plaque located by clicking it in the plaque map. The images are calibrated with voxel intensities and the window and level expressed in density units of mg/cm^3

Automated dual thresholds

Two (2) calcium scoring plaque thresholds are calculated automatically by the N-vivo method, which are patient, scanner, and technique dependent. From within a segmented heart volumetric ROI, the software computes histograms along the z-axis, and calculates blood pool measures which are used to compute the two plaque thresholds for groups of slices along the z-axis of each volumetric CT scan. The high and low thresholds are calculated with density calibrated image voxels as described above and using the equations:

$$HiThreshold = C_1 \times BP(z) + C_2 \times SD(z) + C_3 \tag{1}$$

$$LoThreshold = C_4 \times BP(z) + C_5 \times SD(z) + C_6 \tag{2}$$

where the constants (Cs) are stored in a parameter file of the software; the voxel standard deviations $SD(z)$ and blood pool average densities $BP(z)$ are auto computed from the measured $FWHM(z)$ of the histogram of an auto placed heart volume ROI where $SD(z) = FWHM(z)/2.35$. $BP(z)$ is the computed mean density of voxel intensities bound by the $FWHM(z)$ range and thus excludes voxels in the histogram tails that may contain fat or calcium. Both the noise $SD(z)$ and $BP(z)$ measures are computed along the z-axis to account for patient body size/composition attenuation changes. The N-vivo method is further described elsewhere including details of the auto-computation of the two thresholds [4, 19].

Calcium scoring plaque definitions

The program automatically detects and quantifies individual plaques using the programmed plaque definitions for mass, volume, and Agatston scores. The plaque definition for the calibrated Mass score included 18 point, 3-D voxel connectivity, one voxel $\geq$ the HiThreshold plus 2 additional voxels $\geq$ the LoThreshold, and each voxel calibrated to CaHA concentration densities in mg/cm^3. In addition to the calibrated thresholds, voxel mass and therefore the plaque mass scores were calculated with Hybrid calibrated voxels. The Agatston and volume scores are also automatically calculated by the software using a common Agatston plaque definition ($\geq$130

HU single threshold, 8 pt., 2-D connectivity and 2 pixels for 2.5 mm slices) and allow both calibrated and uncalibrated thresholds.

Automated scoring

The N-vivo software automatically scores plaques satisfying the plaque definitions and patient specific dual thresholds without the operator identifying plaques [19]. The results include the calibrated mass, Agatston (calibrated or uncalibrated) and volume scores for individual plaques, arteries, patient totals, along with the number and mass distribution of plaques. The operator is not required to view each image or manually mark plaques. From the marked origin of the left main coronary artery and its bifurcation at the left anterior descending (LAD) and circumflex (Circ) coronary arteries, the software computes a cylindrical coordinate system and identifies each plaque to its 3-D (x, y, z) location and to one of the major coronary arteries. The detected and measured plaques are then displayed in two plaque maps for the Agatston and mass scores.

CT scans

Patient scans

The patients CT scans were selected from routine calcium scoring studies with no consideration for age or sex. The scans were made with the GE LightSpeed 64 MDCT scanner with 120 kVp, 36 cm FOV, and 350 ms exposures using mA dose modulation and prospective ECG gating at 60%, R-R. A calcium hydroxyapatite calibration phantom was scanned simultaneously with the patients as demonstrated in Fig. 1. All CT scans were scored with both the N-vivo[TM] (calibrated mass) and GE SmartScore[TM] (Agatston) software programs. Scans suspecting to have a zero score were further reconstructed from the same data sets into 0.625 mm slice thicknesses resulting in isotropic voxels ($0.62 \times 0.62 \times 0.62$ mm^3) and the images were sent to the N-vivo workstation connected to the network. Final selection of scans was based on them having a zero calcium score by the conventional Agatston method with 2.5 mm slices. Seventy-eight (78) patient scans were so selected which had a zero Agatston score.

CaHA microsphere phantom scans

A microsphere CCS test phantom was constructed with simulated lung, spine and heart regions as described elsewhere [21]. The phantom contains simulated calcifications manufactured from pure CaHA with microsphere volumes ranging from 0.054 to 3.05 mm^3 and was used to establish ground truth (Fig. 2). The CCS test phantom contains two additional rings to simulate patient sizes. Ten repeat scans were made with a GE LightSpeed 64 MDCT scanner in step and shoot mode with 36 cm FOV, 400 mA and 350 ms exposures. The CCs phantom was also scanned on the C-300 EBCT scanner at 130 kVp and 3 mm slice thickness. The test phantom scans were scored with the automated method using both the mass and Agatston plaque definitions. The measured and calculated masses of microspheres were fit with linear least squares regression equations and Pearson correlation coefficients.

Results

Figure 2 compares images of the CCS Test phantom taken with the C-300 EBCT scanner and with the GE64 MDCT at 2.5 and 0.625 mm slice thicknesses. Only two of the larger targets were scored on the EBCT scan and 4 with the GE64 at 2.5 mm. All 5 of the larger and 5 of the smaller microspheres were scored with 0.62 mm voxels and the N-vivo method. Figure 3 shows the measured mass score of each detected microsphere compared to their known mass. The regression equation for the GE64 2.5 mm slices was omitted to avoid distraction from the measurement points. The smallest microsphere scored with 0.62 mm voxels and the N-vivo method had a volume of 0.075 mm^3.

Figure 4 shows representative clinical images scored by the Agatston and N-vivo methods. All images were constructed from the same scan. Figure 5 shows magnified images of the plaques demonstrated in Fig. 4 to allow better identification of the scored voxels. The small plaque detected only by the use of small voxels and the calibrated mass method contained 15 total connected voxels on three slices and cannot be explained by noise or artifacts. Table 1 summarizes the results for the 78 patient scans. Eighteen (18) of the zero Agatston scores were

Fig. 2 CT images of the
CaHA microspheres in the
CCS Test phantom scanned
with: **a** C-300 EBCT, **b** GE
64 MDCT at 2.5 mm, and
c GE64 0.625 mm slice
thickness. Images (**a**) and
(**b**) show highlighted
microspheres scored by
Agatston and (**c**) shows
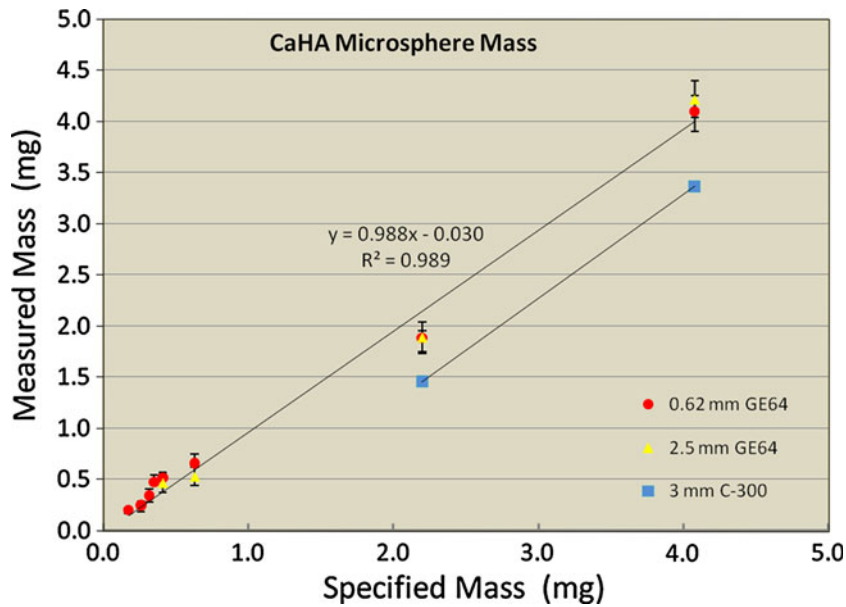those scored by the
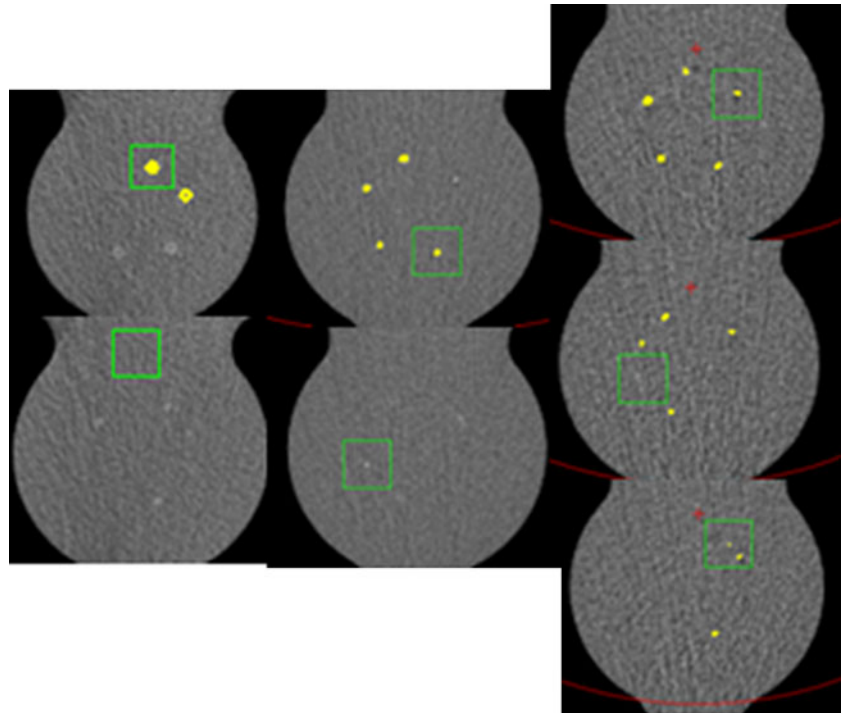calibrated N-vivo™ mass
method

Fig. 3 Measured mass compared to specified mass of the CaHA microspheres of the CCS test phantom. The error bars are ±1 SD measured from 10 repeat scans. The regression equation is for the 0.62 mm reconstructions
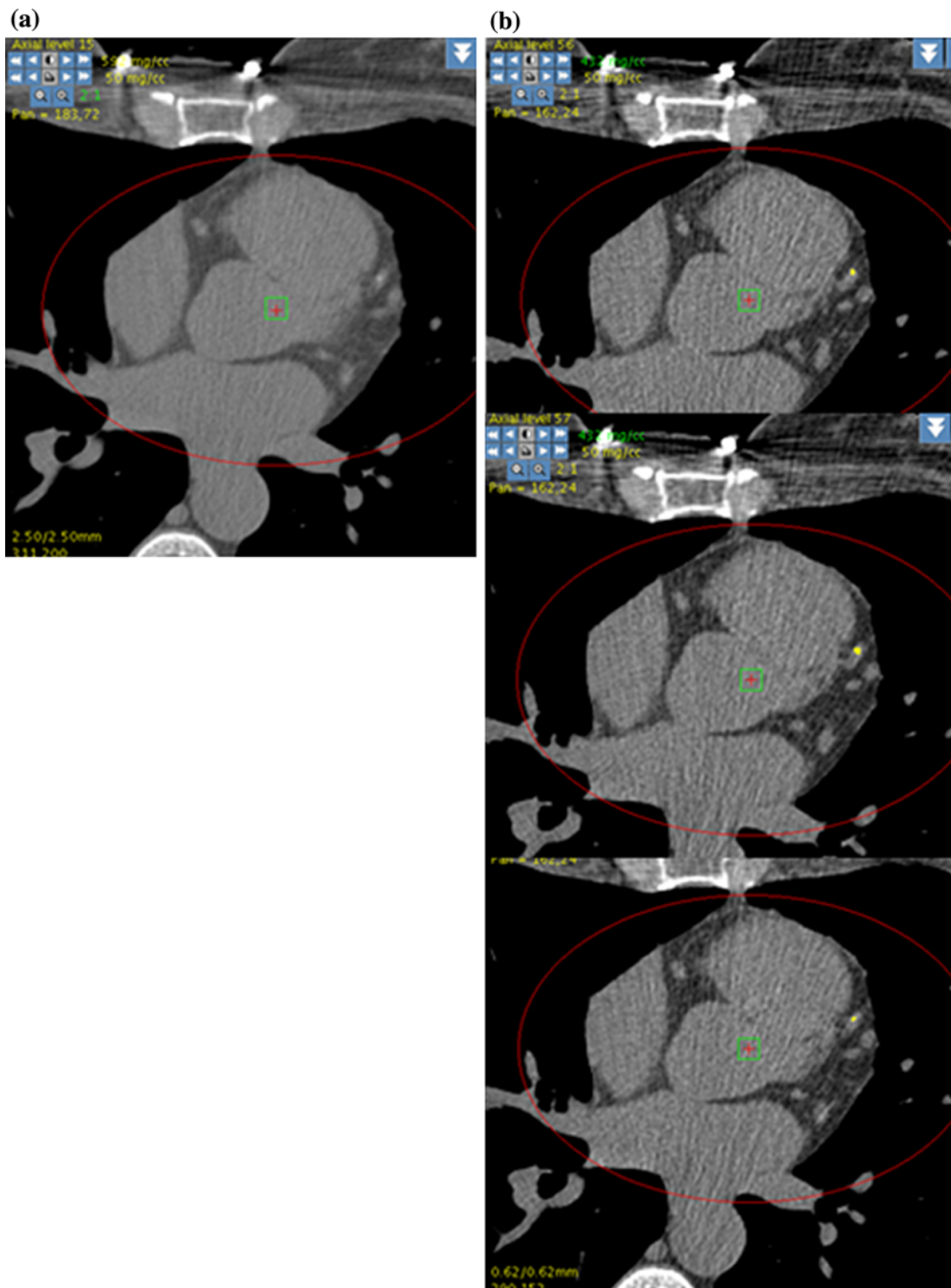
Fig. 4 Example GE 64 MDCT scan reconstructed at 2.5 mm slice thickness and scored by the Agatston method **a** and reconstructed with 0.625 mm slices from the same scan data and scored by the N-vivo method **b**. No calcium was scored with the 2.5 mm voxels while components of the plaque were scored on three adjacent slices at 0.625 mm
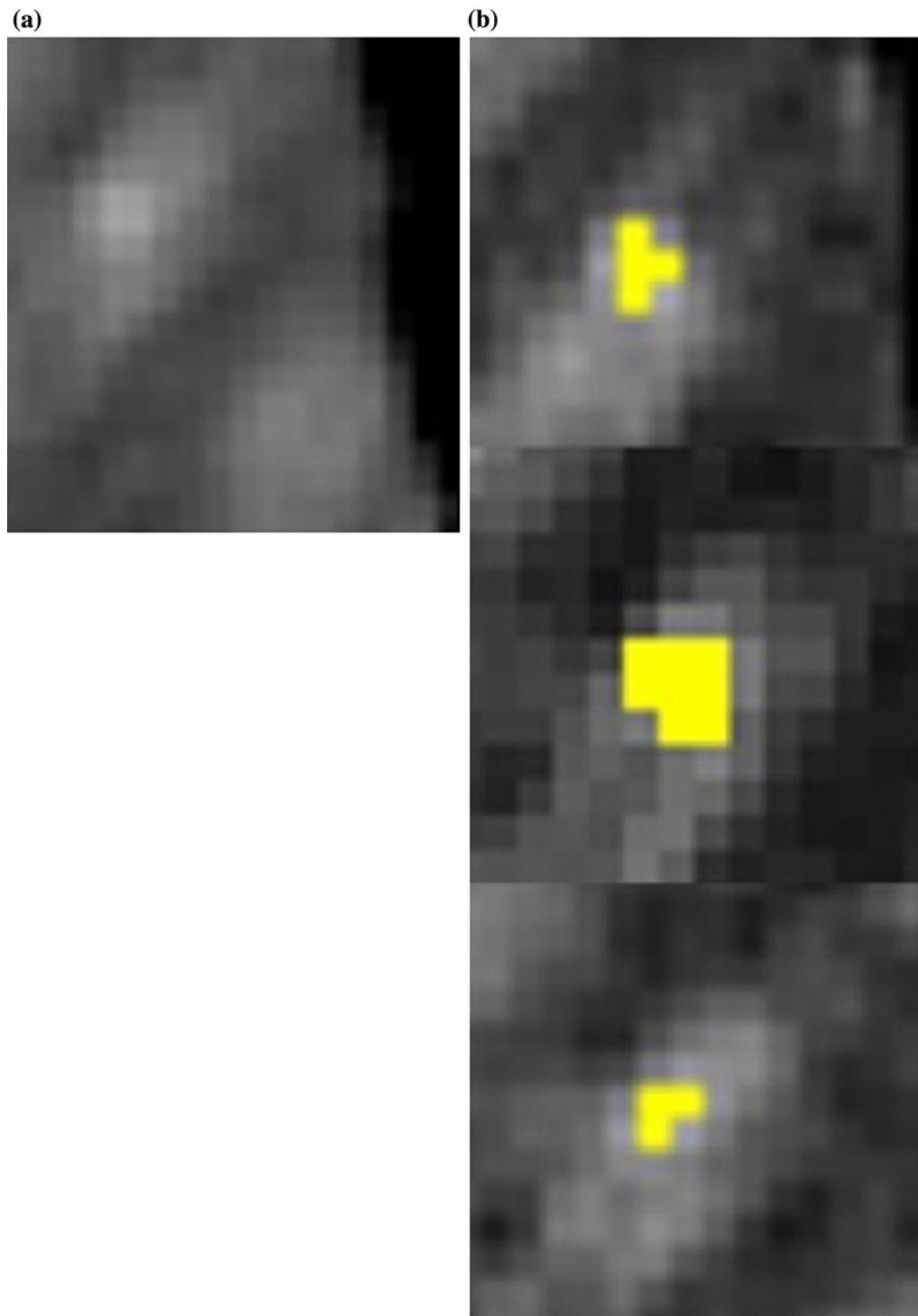
Fig. 5 Magnifications of the plaque regions from Fig. 4. **a** The 2.5 mm image suggests that plaque was present but the signal fell below the Agatston threshold and was not scored. **b** The 0.625 mm images show a total of 15 voxels scored by N-vivo on three slices

Table 1 The number of patients with negative and positive coronary calcium scores by the Agatston and N-vivo methods

	Agatston method	N-vivo method	No of plaque
Negative	78	60	0
Positive	0	18*	1–4

* 18/78 (23%) with negative (zero) Agatston had positive N-vivo mass scores

determined to have small plaque. Most patients showed one detected plaque but some had 2 to 4 small plaques. One patient with a single small plaque experienced an AMI on the table and was sent for stents.

Figure 6 shows CT images also scored by both methods but was not included in the results because the patient had a non-zero Agatston score. Although the one larger plaque was detected and scored by Agatston, six additional very small plaques were detected and scored by the N-vivo method.

Discussion

This study shows that very small coronary calcifications that are missed by current methods can be detected and scored with the advanced method. The phantom validation data shown in Figs. 2 and 3 indicate that very small calcifications, down to about 0.08 mm^3 volumes, can be scored with the new automated method and with high accuracy for mass. This appears to be the first report of scoring such small calcifications by MDCT. The phantom validation also included comparisons of the peak voxel intensities of the microspheres and patient calcifications. The measured maximum noise intensities in the surrounding myocardium were significantly less than the calcium signals as predicted by theory [4]. The use of individual and statistically computed dual thresholds, calibration, and the use of small voxels increased the signal-to-noise allowing the detection of the reduced signals of small calcifications while excluding noise.

Earlier detection of the atherosclerotic process may have important clinical value. It is our hypothesis that very small calcifications are markers for active disease and potentially represent more sensitivity and specific signals for detection and monitoring of atherosclerosis. It may be possible to extract additional diagnostic information by detecting these smaller calcifications

and by more fully characterizing plaque morphology, distribution, and rate of progression. Several studies have established that atherosclerotic lesions are present in coronary sites without significant or even detectable stenosis by angiography. Coronary angiography provides excellent information on vessel obstruction but does not directly provide information on the arterial wall and therefore cannot assess certain important elements of atherosclerosis. In studies of patients suffering acute coronary events verses other high-risk patients who do not, the artery cross-sectional areas by angiography were not significantly different [22–28]. It is also known that most patients suffering AMIs do not have significant vessel stenosis. There is therefore a need to develop additional or more sensitivity tests to identify patients much earlier in the disease process before events occur.

Significant controversy remains on the negative predictive power of a zero calcium score. While some investigators strongly report the diagnostic power of a negative CAC score, others have pointed out the presence of CAD without the presence of detectable coronary calcium [29–31]. Several studies have reported no detectable calcium in some but not most vulnerable plaques as determined by IVUS and/or histological analysis. Other studies report that calcifications are frequently found in ruptured coronary plaques but the presence or absence of calcium is not reliable to discriminate unstable from stable plaques. Budoff et al. [27] has reported a negative predictive power of 98% using CCS to rule out obstructive disease by angiography in a large study. Rosen et al. [29] reported that 4% of MESA participants with a baseline Agatston score of zero were sent for invasive angiography during a median follow-up of 18 months. Others have concluded that a zero calcium score cannot rule out obstructive CAD in symptomatic or young patients [30, 31]. These studies however, all used the current Agatston and large voxel scoring method. It is interesting to note that more recent studies report higher negative predictive powers. We postulate this may be due in part to the use of improved CT scanners and the scoring of smaller calcifications as suggested by the data of Figs. 2 and 3. The summary point of Table 1 is that 23% of our negative Agatston scores had detectable calcifications with small voxel reconstructions and the N-vivo^{TM} method. A recent publication reports manual Agatston scores with 0.5 mm slice thicknesses with similar conclusions to ours [32]. Future work will
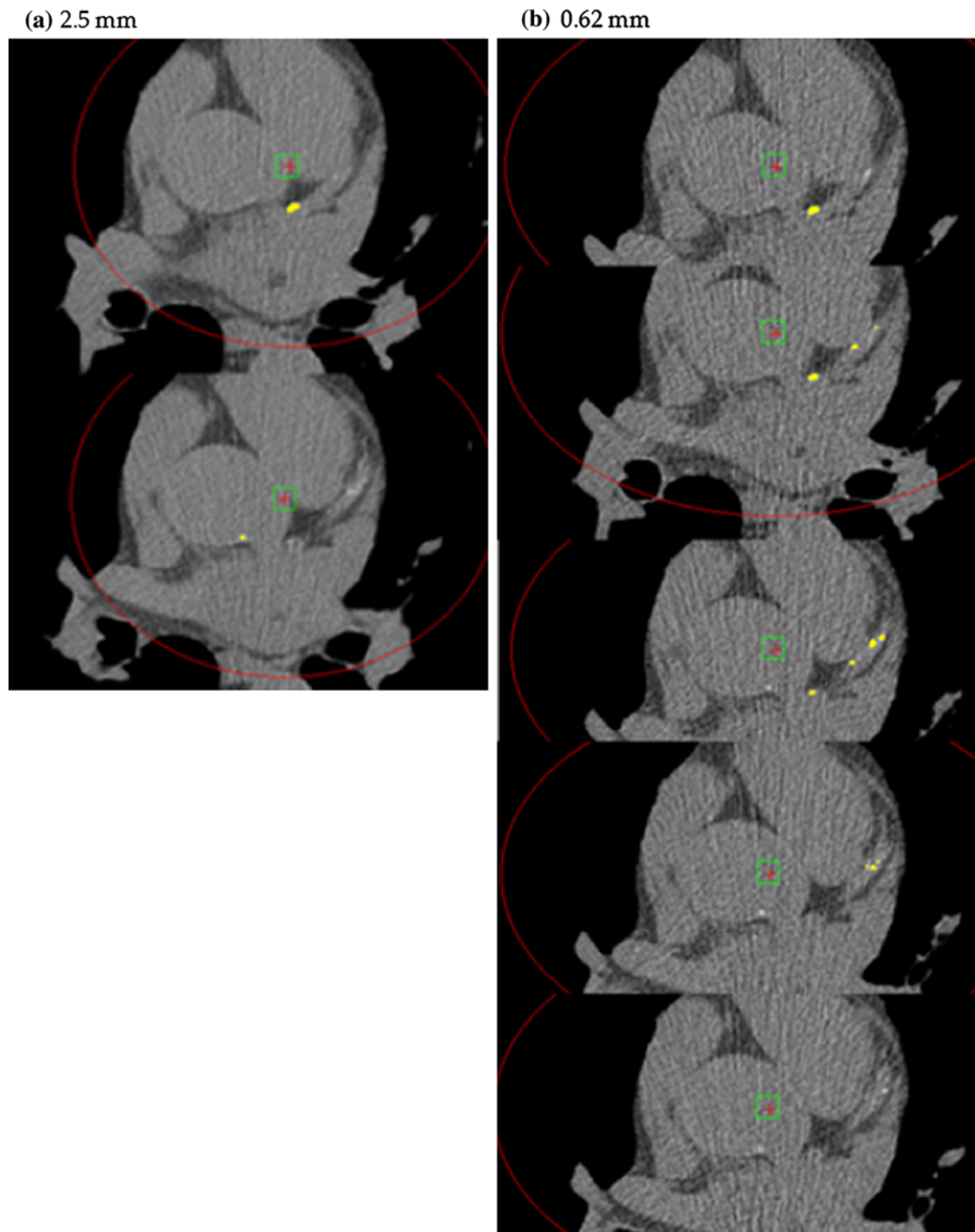
(a) 2.5 mm

(b) 0.62 mm

Fig. 6 GE 64 MDCT images reconstructed from the same scan with 2.5 mm voxels **a** and 0.625 mm voxels **b**. The one plaque detected by Agatston at 2.5 mm had a mass of 7 mg.

The six additional small plaques detected and scored by N-vivo with 0.625 mm voxels had a total mass of 2.1 mg

explore the hypothesis that the current method will improve the negative predictive power to more confidently rule out disease and additional tests. Even in patients with high scores (large calcifications), it is our hypothesis that detection of very small calcifications and quantifying and tracking individual plaques, as opposed to patient 'global scores', will add specificity to the long-term positive predictive power of calcium scoring. Density measurements and analysis of individual plaques have been proposed [33]. We have proposed calibrated mass as the preferred measure for analysis and follow-up of individual plaques [3]. Although individual calcified plaque analysis is suggestive that additional diagnostic information can be extracted, currently no accepted or validated software method is available for such analysis. The current method computes the mass size distribution and displays the plaques in maps to facilitate such a study. Ehara et al. [10] has shown that culprit plaques in coronary arteries are characterized by a spotty pattern of calcifications. The calcification pattern, plaque morphology and remodeling patterns were found to be different between patients with ACS and those with stable conditions. The plaques in the Ehara study were larger as limited by the measurement methods. An important question is whether the detection of smaller calcifications at an earlier time in the disease course may have shown similar or improved discrimination between stable and unstable disease. Our recent work has shown that individual plaque analysis depends heavily on the selected scan parameters, the chosen plaque definitions and the measurement unit. For example, the use of a 2.5 mm slice thickness can lead to neighboring smaller plaques running together to create the perceived measurement of fewer but larger volume plaques of lower densities. The measured densities as well as the Agatston and volume scores show variations between small and large voxels. Figure 6 demonstrates an example where additional small plaques are detected in a patient with larger calcifications successfully scored by the conventional 2.5 mm method. For this patient the number of detected plaques increased from one to seven while the global mass score only increased from 7 to 9.1 mg, i.e. the 6 additional very small plaques total 2.1 mg. It was not the objective of this study to investigate the occurrence of additional small-calcified plaques in patients with confirmed coronary calcium by the Agatston method. However, Fig. 6 suggests such a study is warranted. It

is our hypothesis that the presence of these small plaques increases the risk for future coronary events over and above the global calcium score and their detection may improve the specificity of CCS.

This study has several limitations including the small number of cases and the method of their selection. No other clinical or demographic data were collected on the selected patients to provide any potential insights on the positive cases. The data has not been compared to any other verification methods, such as IVUS or CTA. The data does not provide quantitative results on negative predictive power although improvements are suggested. The data contains no significant information on the incidence rate of patients with very small calcifications or their variations with age and sex.

Conclusions

Calibrated calcium scoring with small voxel CT images and the new automated method increased the detection sensitivity of very small coronary calcifications. The radiation dose was not increased for the small voxels as the images were reconstructed from the exact same scans. Scoring the large number of images produced with thin slices (small voxels) is not practical with conventional manual software. Automated scoring methods such as reported here are therefore required. More definitive clinical and prospective studies are warranted to evaluate the prognostic benefits of higher plaque detection sensitivity and individual plaque analysis.

References

1. Agatston AS, Janowitz WR, Hildner FJ, Zusmer NR, Viamonte M Jr, Detrano R (1990) Quantification of coronary artery calcium using ultrafast computed tomography. J Am Coll Cardiol 15(4):827–832
2. Budoff MJ, Achenbach S, Blumenthal RS, Carr JJ et al (2006) Assessment of coronary artery disease by cardiac computed tomography: a scientific statement from the

American heart association committee on cardiovascular imaging and intervention, Council on cardiovascular radiology and intervention, and committee on cardiac imaging, Council on clinical cardiology. Circulation 114(16): 1761–1791

3. Arnold BA, Budoff MJ, Xiang P, Child J, Mao SS (2009) Detection of very small calcifications by automated coronary calcium scoring with patient specific plaque definitions and hybrid phantom calibration. J Cardiovasc Comput Tomogr 3:S-40

4. Arnold BA, Xiang P, Mao SS, Budoff MJ (2010) Peak SNR in automated coronary calcium scoring: selecting CT scan parameters and statistically defined scoring thresholds. Med Phys 37(7):3621–3632

5. Roijers RB, Dutta RK, Cleutjens PM et al (2008) Early calcifications in human coronary arteries as determined with a proton microprobe. Anal Chem 80(1):55–61

6. Mautner GC, Mautner SL, Froehlich J et al (1994) Coronary artery calcification: assessment with electron-beam CT and histomorphometric correlation. Radiology 192(3): 619–623

7. Rumberger JA, Simons DB, Fitzpatrick LA, Sheedy PF, Schwartz RS (1995) Coronary artery calcium area by electron-beam computed tomography and coronary atherosclerotic plaque area: a histopathologic correlative study. Circulation 92(8):2157–2162

8. Schmermund A, Baumgart D, Mohlenkamp S et al (2001) Natural history and topographic pattern of progression of coronary calcification in symptomatic patients: an electron-beam CT study. Arterioscler Thromb Vasc Biol 21(3): 421–426

9. Sangiorgi G, Rumberger JA et al (1998) Arterial calcification and not lumen stenosis is highly correlated with atherosclerotic plaque burden in humans: a histologic study of 723 coronary artery segments using nondecalcifying methodology. J Am Coll Cardiol 31(3):126–133

10. Ehara S, Kobayashi Y et al (2004) Spotty calcification typifies the culprit plaque in patients with acute myocardial infarction: an intravascular ultrasound study. Circulation 110(22):3424–3429

11. Schmid K, McSharry WO, Pameijer CH et al (1980) Chemical and physicochemical studies on the mineral deposits of the human atherosclerotic aorta. Atherosclerosis 37(2):199–210

12. Virmani R, Burke AP, Kolodgie FD, Farb A (2003) Pathology of the thin-cap fibroatheroma. J Interv Cardiol 16(3):267–272

13. Friedrich GJ, Moes NY, Muhlberger VA, Gabl C, Mikuz G, Hausmann D, Fitzgerald PJ, Yock PG (1994) Detection of intralesional calcium by intracoronary ultrasound depends on the histologic pattern. Am Heart J 128(3): 435–441

14. Leber AW, Becker A, Knez A et al (2006) Accuracy of 64-slice computed tomography to classify and quantify plaque volumes in the proximal coronary system, a comparative study using intravascular ultrasound. J Am Coll Cardiol 47(3):672–677

15. Leber AW, Knez A, Becker A, von Ziegler F, Nikolaou K, Rist C, Reiser M, White C, Steinbeck G, Boekstegers P (2004) Accuracy of multidetector spiral computed tomography in identifying and differentiating the composition of coronary atherosclerotic plaques: a comparative study with intracoronary ultrasound. J Am Coll Cardiol 43(7):1241–1247

16. Achenbach S, Moselewski F, Ropers D, Ferencik M, Hoffmann U, MacNeill B, Pohle K, Baum U, Anders K, Jang IK, Daniel WG, Brady TJ (2004) Detection of calcified and noncalcified coronary atherosclerotic plaque by contrast-enhanced, submillimeter multidetector spiral computed tomography: a segment-based comparison with intravascular ultrasound. Circulation 109(1):14–17

17. Rasouli ML, Shavelle DM, French WJ, McKay CR, Budoff MJ (2006) Assessment of coronary plaque morphology by contrast-enhanced computed tomographic angiography comparison with intravascular ultrasound. Coron Artery Dis 17(4):359–364

18. Arnold BA (2007) Calibration of tissue densities in computerized tomography. US Patent No: 7,292,721

19. Arnold BA, Reed J (2009) Automatic detection and quantification of coronary and aortic calcium. US Patent No: 7,558,611

20. McCollough CH, Kaufmann RB, Cameron BM, Katz DJ, Sheedy PF, Peyser PA (1995) Electron-beam CT: use of a calibration phantom to reduce variability in calcium quantization. Radiology 196(1):159–165

21. Arnold BA, Matthew J, Budoff MJ, Child J, Ping Xiang P, Song S, Mao SS (2010) Coronary calcium test phantom containing true CaHA microspheres for evaluation of advanced CT calcium scoring methods. J Cardiovasc Comput Tomogr 4(5):322–329

22. Haber R, Becker A, Leber A et al (2001) Correlation of coronary calcification and angiographically documented stenoses in patients with suspected coronary artery disease: results of 1, 764 patients. J Am Coll Cardiol 37(2):451–457

23. Hoffmann U, Moselewski F, Nieman K, Jang I-K, Ferencik M, Rahman AM, Cury RC, Abbara S, Joneidi-Jafari H, Achenbach S, Brady TJ (2006) Noninvasive assessment of plaque morphology and composition in culprit and stable lesions in acute coronary syndrome and stable lesions in stable angina by multidetector computed tomography. J Am Coll Cardiol 47(8):1655–1662

24. Knez A, Becker A, Leber A et al (2004) Relation of coronary calcium scores by electron beam tomography to obstructive disease in 2, 115 symptomatic patients. Am J Cardiol 93(9):1150–1162

25. Budoff MJ, Raggi P, Berman D et al (2002) Continuous probabilistic prediction of angiographically significant coronary artery disease using electron beam tomography. Circulation 105(15):1791–1796

26. Rumberger JA, Schwartz RS, Simons DB, Sheedy PF III, Edwards WD, Fitzpatrick LA (1994) Relation of coronary calcium determined by electron-beam computed tomography and lumen narrowing determined by autopsy. Am J Cardiol 73(16):1169–1173

27. Budoff MJ (2006) Prevalence of soft plaque detection with computed tomography. J Am Coll Cardiol 48(2):319–321

28. Moselewski F, Ropers D, Pohle K, Hoffmann U, Ferencik M, Chan RC, Cury RC, Abbara S, Jang IK, Brady TJ, Daniel WG, Achenbach S (2004) Comparison of measurement of cross-sectional coronary atherosclerotic plaque and vessel areas by 16-slice multi detector computed tomography versus intravascular ultrasound. Am J Cardiol 94(10):1294–1297

29. Rosen BND, Fernandes V, McClelland RL, Carr JJ, Detrano R, Bluemke DA, Lima JAC (2009) Relationship between baseline coronary calcium score and demonstration of coronary artery stenoses during follow-up: MESA (multi-ethnic study of atherosclerosis). JACC Cardiovasc Imaging 2(10):1175–1183
30. Rubinshtein R, Gaspar T, Halon DA, Goldstein J, Peled N, Lewis BS (2007) Prevalence and extent of obstructive coronary artery disease in patients with zero or low calcium score undergoing 64-slice cardiac multidetector computed tomography for evaluation of a chest pain syndrome. Am J Cardiol 99:472–475
31. Marwan M, Ropers D, Pflederer T, Daniel WG, Achenbach S (2009) Clinical characteristics of patients with obstructive coronary lesions in the absence of coronary calcification: an evaluation by coronary CT angiography. Heart 95:1056–1060
32. Van der Bijl N, de Bruin PW, Geleijns J, Bax JJ, Schuijf JD, de Roos A, Kroft LJM (2010) Assessment of coronary artery calcium by using volumetric 320-row multi-detector computed tomography: comparison of 0.5 mm with 3.0 mm slice reconstructions. Int J Cardiovasc Imaging 26(4):473–482
33. Moselewski F, O'Donnell CJ, Achenbach S, Ferencik M, Massaro J, Nguyen A, Cury RC, Abbara S, Jang I-K, Brady TJ, Hoffmann U (2005) Calcium concentration of individual coronary calcified plaques as measured by multidetector row computed tomography. Circulation 111(24):3236–3241